Dynamics and growth patterns of calcareous sponge spicules

MICHA ILAN[1], JOANNA AIZENBERG[2] AND OSNAT GILOR[1]

[1] *Department of Zoology, Tel Aviv University, Tel Aviv 69978, Israel*
[2] *Department of Structural Biology, Weizmann Institute of Science, Rehovot 76100, Israel*

SUMMARY

Morphogenesis of different-shaped biogenic crystals presents one of the important biomineralization problems. Growth of various calcitic spicules from *Sycon* sp. have been studied by using calcein marking. We found that spicule production is dependent on various conditions such as location in the sponge body and illumination, whereas the calcification rate by the spicule-forming cells is constant. Morphological, crystallographic and fluorescence analyses have enabled the investigation of the growth patterns of the different spicule types. We suggest that different mechanisms are involved in the growth of various spicule types. Triradiate spicules are deposited from the centre towards the rays. Crystallographically different rays of the triradiates differ in the dynamics of formation as well. Slender monaxon spicules are deposited very fast (more than 65 μm/h). Two calcification sites are involved in the secretion of curved monaxon spicules. These spicules grow unidirectionally from one extremity at a rate of 12.0 μm/h, and are thickened at some distance from the nucleation site. Possible mechanisms that may account for the observed growth patterns are discussed.

1. INTRODUCTION

Organisms use a wide variety of mineralized tissues for constructing their skeletal hard parts. One skeletal connective tissue type is composed of mineral spicules embedded in a pliable organic matrix. Such connective tissues can be found in many phyla, including sponges, cnidarians, molluscs, echinoderms and urochordates (Simkiss & Wilbur 1989). They are for the most part composed of calcite or silica and have a remarkable range of morphologies that are quite different from their mineral counterparts of inorganic origin. Despite their wide distribution in the animal kingdom, many aspects of spicule formation remain unclear: the identity and number of the cells which deposit the spicule and how they control spicule shape; is the process localized within the organism; what is the rate of spicule deposition and its relation to the conditions of illumination?

The sponges (Porifera) are among the most primitive of animal phyla. Their highly controlled spicule mineralization processes may help us better understand a wide spectrum of biomineralization problems. Species in the class Calcarea attracted our attention, because they possess a connective tissue skeleton which contains a variety of differently shaped spicules, each of which is a single crystal of Mg-bearing calcite (Minchin 1898).

The structure, composition and development of calcareous sponge spicules have been subjects of discussion for the past 100 years (Ebner 1887; Minchin 1909; Jones 1970; Ledger & Jones 1977, 1991). It was established that sponge spicules are secreted by cells termed sclerocytes. Minchin (1909) concluded that one cell (which he termed the 'founder cell'), is responsible for the formation and elongation of the monaxon spicule. Another cell (the 'thickener cell') is responsible for the thickening of the spicule. Ebner (1887), in contrast, invoked a concentric three-dimensional growth of the monaxon spicule from its centre. Triradiate spicule formation follows the assembly of three pairs (sextet) of sclerocytes. Originally it was suggested that the three rays of the triradiates are deposited separately, as non-birefringent rodlets which later fuse together (Minchin 1898). Ultrastructural studies of cell formation and movements showed that these observations were probably erroneous, concluding that the initial calcite is most probably deposited within the centre of the sextet, and then the rays grow outward (Jones 1970; Ledger & Jones 1977). The development of triradiates from the centre to the tip of the rays has not, however, been shown unequivocally. We recently suggested a mechanism of control over spicule shape and crystallographic orientation involving oriented nucleation followed by unidirectional crystal growth. The latter may be achieved through either physical or stereochemically driven adsorption of specialized macromolecules introduced into the microenvironment of spicule growth (Aizenberg *et al.* 1995*a*, *b*).

Another possible way to study skeletal deposition is by fluorescent labelling of the growing crystals. Bavestrello (1993) examined the formation of triradiates by the use of tetracycline. However in all cases, spicule production ceased after 24 h. Because tetracycline may have deleterious effects on the organisms (Levin 1990), alternative harmless markers like calcein, are preferable.

Proc. R. Soc. Lond. B (1996) **263**, 133–139
Printed in Great Britain

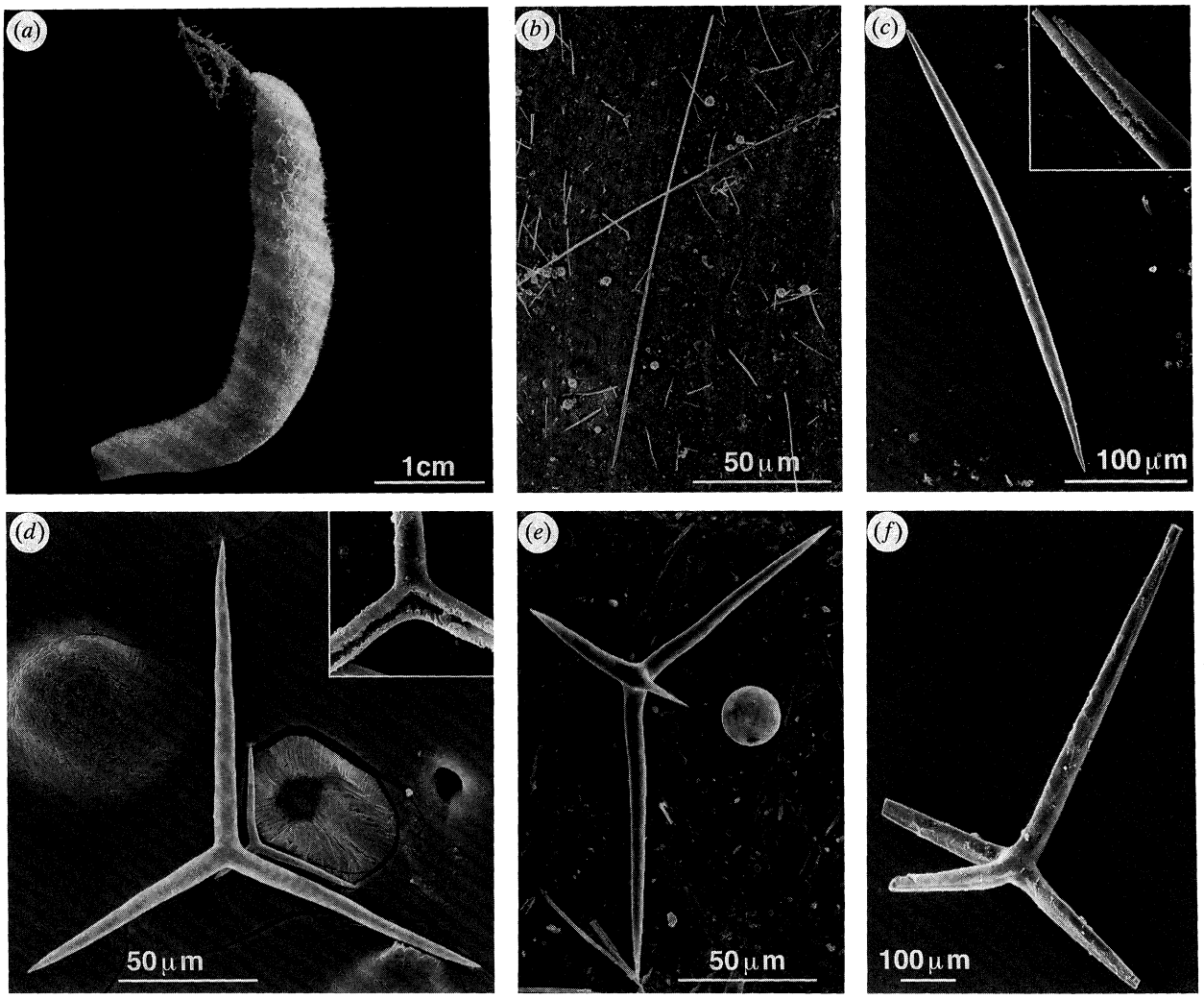

Figure 1. The calcareous sponge *Sycon* sp. and the various spicule types formed by it. (*a*) The intact sponge in its natural, upside down, position. (*b*) Slender monaxons. The spicules are elongated along *c*-axis; (*c*) A curved monaxon spicule. The approximate direction of elongation is [012]. Insert: partially etched spicule, showing two mineral rods enveloped by the calcitic sheath. (*d*) Triradiate spicules. Insert: partially etched triradiate, showing the similarity in the structure between the two paired rays of the triradiate and the curved monaxons. (*e*) A quadriradiate spicule. The directions of elongation of the three long rays correspond to those of the triradiate spicule. The fourth ray is short and curved. (*f*) A giant quadriradiate spicule from the external surface. Except for (*a*) all are scanning electron micrographs.

In this work we extend our studies of the mechanisms of formation of calcareous sponge spicules to determine and compare the growth patterns of various spicule types within a single calcareous sponge by using calcein labelling. The aspects examined were: the rate of spicule elongation; the growth pattern (direction) of differently shaped spicules; a comparison of the proportion of spicules deposited in different body regions; and the effect of absence of light on spicule calcification.

2. MATERIALS AND METHODS

(*a*) *Sponge collection*

Sponges were collected off floating docks (Friday Harbor Laboratories, Washington). They grow in an upside down position, clustered in well illuminated sites, but never exposed to direct light. Sponges 3–5 cm long were collected still attached to small pieces of their substrate, gently cleaned, and transferred to the laboratory without being exposed to air. Species identification follows Laubenfels (1961), and Austin & Ott (1987).

(*b*) *Experimental set-up*

Four jars, each filled with three litres of sand-filtered seawater containing 125 mg/l calcein (Sigma) were gently stirred with Plexiglas Paddles attached to a small rotary motor (for description see Strathmann 1987). The jars were held within a waterbath filled with running seawater at ambient seawater temperature. Two of the jars were wrapped all-over with aluminum foil for complete darkness 24 h/day (D), whereas the two other jars were exposed to light 12 h, followed by 12 h in darkness (L). Eight animals were put in each jar. Three hours later, two animals were gently removed from each treatment and put into a beaker filled with 0.22 μm filtered seawater. After

30 min all the excess calcein was rinsed out of the sponges, by their natural water pumping activity. The sponges were then removed, rinsed in distilled water for a few seconds, put on paper towel to absorb the excess water, and immediately transferred to −20 °C. The process was repeated with other specimens after 24 h and 55 h from the beginning of the experiment. Six samples were obtained (3D, 3L, 24D, 24L, 55D, 55L) frozen, freeze-dried and maintained sealed until further treatment.

(*c*) *Spicules examination*

For preliminary information, the freeze-dried sponges were observed intact using an epi-fluorescence microscope (Zeiss 16), and after gold-coating in the scanning electron microscope (JEOL 6400) (SEM). Two samples were then taken from each of six specimens, one from around the osculum (the sponge's distal opening) (O), and one from the central part of the body (C). The mechanisms of spicule deposition were studied separately in the twelve different samples obtained that correspond to the various experimental conditions (3LC, 3LO, 3DC, 3DO, 24LC, 24LO, 24DC, 24DO, 55LC, 55LO, 55DC, 55DO). For further examination, the spicules from each specimen were extracted and cleaned by immersion in 2.5% NaOCl solution for 10 min. Sodium hypochlorite was removed by centrifugation and the liberated spicules were washed several times in double distilled water and finally in absolute ethanol. Clean spicules were placed on a glass slide and examined by fluorescence microscopy. The orientations of the spicule crystallographic axes were deduced from polarized light studies and crystal decoration (Okazaki *et al.* 1981). Measurements of the length of the fluorescent and non-fluorescent parts of the spicules were taken from photographs (20–40 fluorescent spicules were used for each experimental condition). The extent to which label penetrates into the spicule was estimated by selective etching of the fluorescent regions using mild solutions of HCl (pH = 6) and/or KOH (pH = 9).

3. RESULTS

(*a*) *General description*

In life the colour of the sponge is dirty white to beige, and it has a soft consistency. The sponge surface is minutely hispid to the naked eye, with no apparent coronal fringes. Microscopical examination, however, revealed such coronal fringes. The choanocytes are arranged in a syconoid pattern. The sponge was identified only as *Sycon* sp. (figure 1*a*). It does not resemble *S. compactum* (Lambe 1893) or *S. raphanus* (Schmidt 1862) reported from this location (Laubenfels 1961).

The sponge deposits five main types of spicules: two forms of monaxons, two forms of quadriradiate and one triradiate. All the spicules are birefringent in polarized light. The slender monaxons (SMX) form a well-developed fringe near the oscular region, and are not found elsewhere in the sponge. They reach 200 μm in length and 2–3 μm in thickness (figure 1*b*). Each SMX

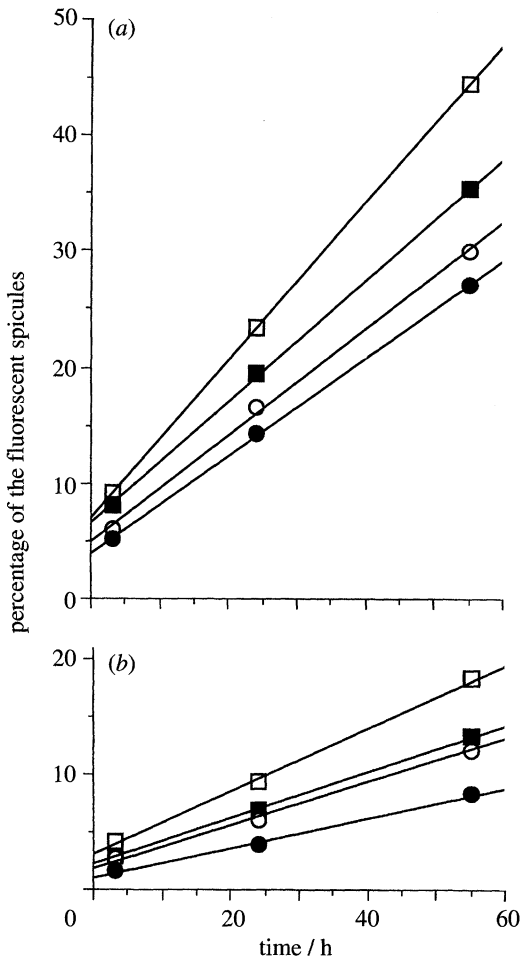

Figure 2. Percentage of the fluorescent spicules in the total spicule population within sampling time intervals for different experimental conditions. (*a*) Curved monaxon spicules. (*b*) Triradiate spicules. D – samples studied under continuous darkness; L – samples exposed to light; C – samples from the central part of the sponge body; O – oscular vicinity. Linear fit is used, $R^2 \geqslant 0.99$ in every case. Filled circles = DC; filled squares = DO; hollow circles = LC; and hollow squares = LO.

is composed of a single straight calcitic rod. The orientation of its *c* crystallographic axis coincides with the direction of spicule elongation.

Curved monaxons (CMX) are present both near the osculum and in the central part of the sponge body. They are 200–400 μm long and 5–10 μm thick (figure 1*c*). About 80–120 μm of the CMX protrude from the tissue forming the hispid sponge surface. The outer ends are often slightly etched. Unlike the SMX, the etched CMX clearly reveal two body rods covered together by an additional mineral layer that envelops the entire spicule. The c crystallographic axis forms a constant angle of about 65 ° with the direction of the spicule morphological axis.

Triradiates, like CMX, are also deposited all around the sponge body (figure 1*d*). They are entirely embedded within the sponge body forming highly oriented arrays. The triradiates have a wide size distribution (50–100 μm). Their rays are unequal. Two rays (so-called paired rays) are slightly curved and have the same appearance and crystallographic

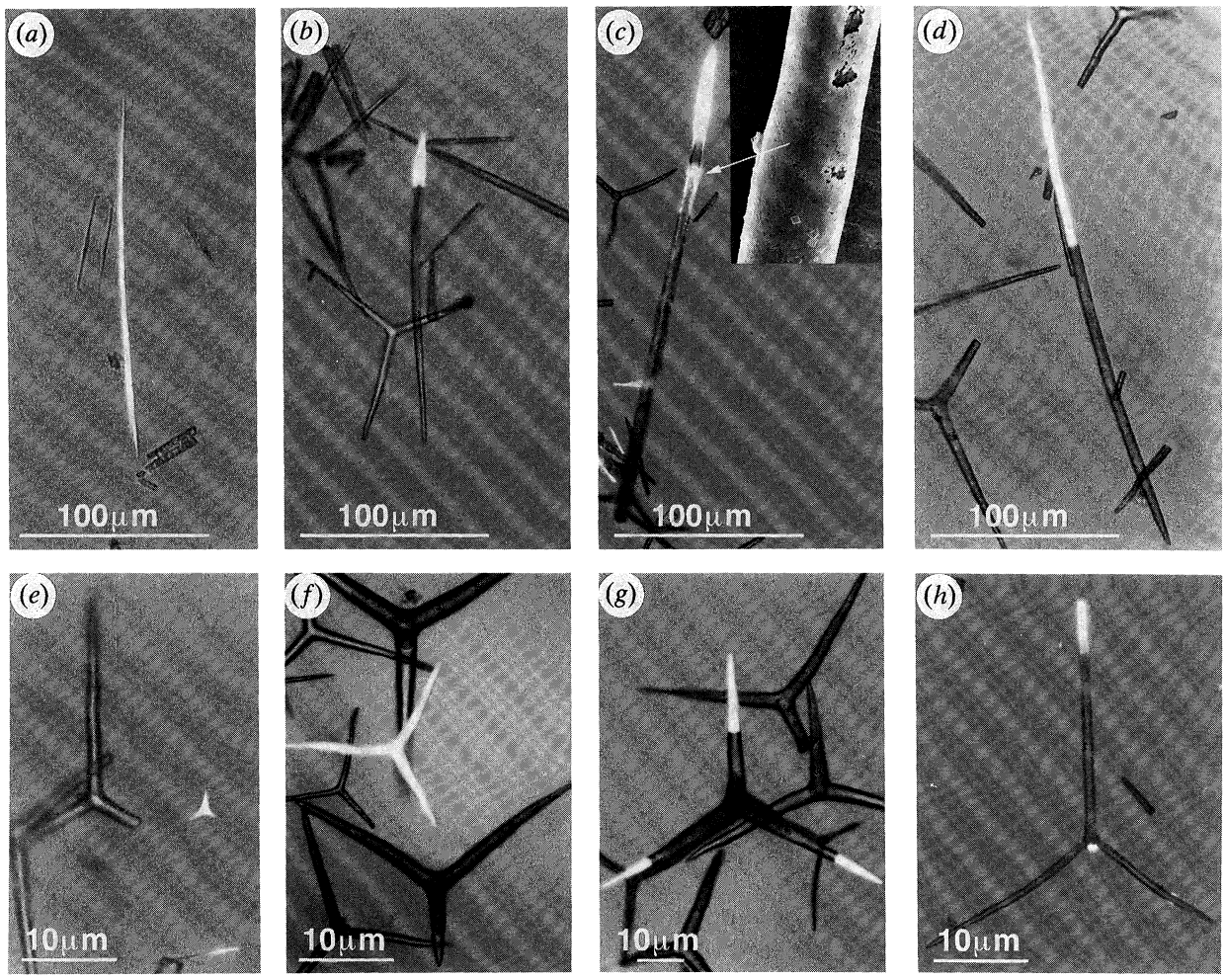

Figure 3. Fluorescent spicules of different types. (*a*) A slender monaxon after 3 h of the calcein treatment. (*b*) A curved monaxon after 3 h of the calcein treatment. Note that calcification takes place from one spicule tip. (*c*) A curved monaxon after 24 h of immersion in calcein. An additional fluorescent band at some distance from the growing end is evident. Insert: A scanning electron micrograph of the fluorescent area of the same spicule. Note the thickening that occurs on the band location. (*d*) A curved monaxon after 55 h of immersion in calcein. Note that two fluorescent regions overlap. (*e*) A newly-formed triradiate spicule. (*f*) A triradiate spicule entirely formed within 24 h. (*g*) A triradiate spicule with growing extremities of the rays. (*h*) A quadriradiate spicule. Note that mineral deposition occurs only on the fourth ray and extremity of the unpaired ray. The photographs were taken using fluorescent and white light.

orientation as the CMX. The third, unpaired, ray is straight, and resembles the SMX both morphologically and crystallographically. The triradiates occasionally display a fourth ray, thus having the appearance of the regular quadriradiates (figure 1*e*). The fourth apical ray is short (10–20 μm) and usually highly curved. The sponge external surface is regularly meshed and reinforced by the giant quadriradiates (500–700 μm) (figure 1*f*).

(*b*) *Dynamics of spicule formation*

The sponge oscula, fringed by SMX, were highly fluorescent in all the specimens even after 3 h of the calcein treatment. However, the other external parts of the sponges showed no fluorescence in the samples exposed to calcein for 3 h and 24 h. In all the specimens kept in calcein for 55 h, slight fluorescence was observed in the protruding spicule extremities.

Although CMX and triradiates are being deposited all around the sponge body, more are deposited closer to O than in C (figure 2). More fluorescent spicules (CMX and triradiates) are produced in the specimens exposed to light as compared with those grown under dark conditions. The percentage of growing triradiates is generally 2–3 times smaller than that of CMX.

(*c*) *Spicule growth patterns*

Even within 3 h of immersion most of the SMX were completely marked (figure 3*a*). Fluorescence was observed at each stage during the progressive etching of the marked spicules, suggesting that every SMX is deposited entirely within this short period of time.

Curved monaxons have three prominent fluorescence patterns: (i) only one extremity of the marked spicules is fluorescent (figure 3*b*); (ii) the extremity and an additional narrow fluorescent band is evident, about 80–100 μm toward the spicule's centre (figure 3*c*); and (iii) about 50% of the spicule is marked, and no additional band is present (figure 3*d*). The first pattern is observed after 3 h of immersion in calcein.

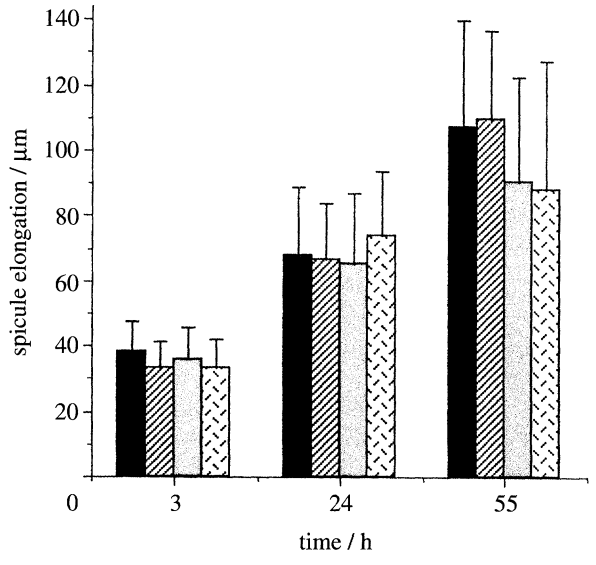

Figure 4. Average elongation of curved monaxon spicules after different time intervals. D – samples studied under continuous darkness; L – samples exposed to light; C – samples from the central part of the sponge body; O – oscular vicinity. The error bars represent standard deviation of spicule elongation within the same individual (20–40 spicules for each condition). Note that the elongation is independent of the conditions of examination. Black shading = DC; stripes = DO; grey shading = LC; other = LO.

The second is dominant for spicules kept in calcein for 3–24 h. The third pattern is observed after 55 h of calcein treatment. It is noteworthy, that the CMX are slightly thicker in the band location (figure 3*c*, insert). The fluorescent band is easily removed after the very first steps of spicule etching, indicating an addition of a thin mineral layer to the earlier deposited spicule. In contrast, the fluorescent layer of the growing extremities cannot be removed by partial etching, implying that an entire growing end was newly deposited during the time of immersion. No difference in the lengths of the apical growing regions exists between the four samples (D versus L, and O versus C) within every studied time interval (figure 4).

The fluorescence pattern of triradiates consisted of completely marked very small (3–5 μm across) and larger (10–50 μm across) spicules (figure 3*e*), as well as mature spicules in which only the distal parts of all the rays, or just of the unpaired ray, were marked (figure 3*f*). Even after gradual etching, none of the spicules were observed to have fluorescence in the central part with unmarked extremities of the rays.

Only very few quadriradiates were fluorescent, which hampered any quantitative analysis of the process. Qualitatively, however, the observations revealed that in the few spicules with fluorescence, the mark was usually on the fourth, much smaller, ray. The giant external quadriradiates showed no fluorescence.

(*d*) *Growth rate*

We could estimate only the lower limit of the growth rate of SMX (more than 65 μm/h), as within 3 h their entire length (200 μm) was marked. Because no significant difference in length increment of CMX was found either between C and O or L and D (figure 4), the data for every studied time interval were pooled. The calculated mean elongation were 36 ± 9 μm per 3 h; 69 ± 20 μm per 24 h and 95 ± 36 μm per 55 h which gives the mean growth rates of 12 ± 3 μm/h, 2.9 ± 0.8 μm/h, and 1.7 ± 0.7μm/h respectively. Growth of CMX between time intervals is demonstarted in figure 4.

4. DISCUSSION

We have shown here that the growth patterns of the various spicule types differ, and that spicule production is dependent on the location within the sponge body and on the conditions of illumination. Clearly, spicule formation in calcareous sponges presents many fascinating problems related to skeletal morphology determination, as well as to the dynamics and directions of biological crystal growth.

Calcein was found to be a suitable marker to study calcareous sponge spiculogenesis. Calcification proceeded during the 55 h of examination, in contrast to the deleterious effect observed during sponge immersion in tetracycline (Bavestrello *et al.* 1993). The fact that after 3 h and 24 h the sponge external surface is not fluorescent (except for the oscular fringe), demonstrates that calcein is incorporated into the spicules as a result of biological activity, and is the result of uncontrolled adsorption of calcein on exposed spicule surfaces. This non-invasive, non-toxic or minimally toxic method is suggested to be better than tetracycline marking in calcification studies of this type.

An evaluation of the minimal rate of spicule formation can be made from the 3 h calcein pulse labelling experiment. Spicule growth rates calculated from longer time points underestimate the real growth, because they also include spicules whose calcification ceased before or started toward the end of the marking period. Curved monaxons elongate at a constant rate of 12 ± 3 μm/h, irrespective of the location in the sponge body or conditions of illumination (figure 4). This is much faster than in *Leucosolenia variabilis* (3.78 μm/h, Jones 1970) but only slightly faster than in *Sycon ciliatum* (8.85 μm/h, Jones 1979). Such growth rate suggests that the entire CMX might be secreted within 17–33 h. Indeed, among the spicules examined after 55 h, we found several CMX which were completely marked. A very fast average deposition rate of more than 65 μm/h was found for the slender monaxons, that were all entirely formed within the shortest period of observation.

It is evident that most spicules are formed in the oscular vicinity. Only slender monaxons are deposited just in this location, and more curved monaxons and triradiates are produced near the osculum as compared with the central part of the body (figure 2). This region is the growing front of the sponge which enlarges mainly along its longitudinal axis. A smaller proportion of newly-formed spicules are present in the central part of the sponge, where growth widens the sponge body.

This can be indicative of the differences either in the amount of sclerocytes or their activity in the different regions within the sponge body. However, the rate of spicule elongation is independent of the sclerocyte location. The amount of spicules deposited can, therefore, differ between various body regions, and sampling of a specific region may misrepresent the complete picture.

No apparent delay in calcification rate was observed under dark conditions for this species, in contrast to reports from other calcareous sponges (Bavestrello *et al.* 1993). Unlike 'light enhanced calcification' in scleractinians, which has been attributed to the zooxanthellae activity (Ruppert & Barnes 1994), the rate of spicule growth of *Sycon* sp. under different conditions of illumination is the same. However, there is a production of more spicules under normal light regime compared to that in continuous darkness (figure 2). This difference may indicate that more sclerocytes become active and are engaged in calcification when the specimens are exposed to light, but their calcification rate is constant.

This study clearly shows that different spicules exhibit different growth patterns. Formation of the triradiates has been a subject of much controversy as to whether they grow continuously from the centre, or they arise from the three individual rays that fuse together (Minchin 1898; Jones 1970). We show that they initially form a small triangular nucleus (figure 3*e*), and then grow to become small triradiates (figure 3*f*). We also observed triradiates which were completing their deposition when immersed in a calcein solution, and were marked only at the ray tips (figure 3*g*). Furthermore, as no fluorescence was observed in the central parts of the spicules with unmarked extremities of the rays, we can unequivocally conclude that the triradiates do not arise from initial growth of the three separate rays, but are deposited from the centre towards the rays. It is noteworthy that the growth dynamics of two paired rays of the triradiates are different from that of the third, unpaired, ray. This is consistent with the observed differences in crystallographic orientation and appearance (figure 1*d*). This conclusion is based on our common observation of the ongoing calcification of the unpaired ray, after the two other rays have completed their growth (figure 3*h*). In the regular quadriradiates, the last ray to be deposited is the usually small, occasionally deformed ray as predicted by Jones (1970). We stress that the triradiates are arranged in ordered arrays with their unpaired rays preferentially oriented such that they are parallel to each other. This may provide the organism with some advantageous mechanical properties (Koehl 1982).

Slender monaxons which form the fringe around the osculum are markedly different from other spicule types with respect to rate of spicule deposition. The fast rate of spicule deposition may serve the need for rapid spicule replenishment. The elongated morphology of these rapidly growing crystals may be achieved by a highly directional transport of calcium ions in the axial direction. As a result, the spicule is pushed out through the membrane by a very strong flux of ions. This mechanism also explains the preferred spicule elongation along the crystallographic *c*-axis, which corresponds to the direction of the fastest growth of calcite crystals.

A different mechanism of anisotropic growth appears to be present in the curved monaxons. We show that deposition occurs from the one spicule extremity located within the sponge body, followed by unidirectional growth towards the sponge external surface (figure 3*b–d*). This is in agreement with the mechanism proposed by Aizenberg *et al.* (1995*b*). Thickening of the spicule and formation of the thin separate fluorescent band at some distance from the distal growing tip, indicate that additional calcification takes place during crystal growth. These observations differentiate between two contradicting descriptions of spicule growth pattern which exist: the concentric spicule growth (Ebner 1887) or the unidirectional growth (Minchin 1909). We suggest that the apical cell forms a primary nucleation site. Its organization and ultrastructure controls nucleation off the (012) calcite face. The second (thickener) cell serves a need for a spatial constraint of the lateral growth. It adds an external layer and 'smoothes' the spicule into its final shape. This cell may generate a specific microenvironment that provides the directional flux of ions and proteins towards the crystal surface. Similar mechanisms of control over biogenic crystal growth were proposed for other organisms (Mann *et al.* 1987; Mann & Sparks 1988). A particular spicule form is therefore the outcome of the directing and molding activities of the spicule-forming cells.

Some common mechanisms are involved in the formation of sponge spicules, though insufficient number of different morphological types have been studied to date, and related to the ultrastructure of the surrounding organic material. The same relations might be valid in other phyla which deposit minerals. A careful study of this group could therefore shed light upon biomineralization questions of much wider significance, because many aspects of crystal organization, development and structure, which in other animals are extremely complicated, are more accessible in sponges.

We thank S. Weiner and L. Addadi for suggestions throughout the spicules analysis and for critically reviewing the manuscript. We appreciate the help and hospitality of the staff of Friday Harbor Laboratories and especially R. R. Strathmann and M. F. Strathmann.

REFERENCES

Aizenberg, J. Hanson, J. Ilan, M. *et al.* 1995*a* Morphogenesis of calcitic sponge spicules: a role for specialized proteins interacting with growing crystals. *FASEB* **9**, 262–268.

Aizenberg, J. Hanson, J. Koetzle, T. F. *et al.* 1995*b* Biologically induced reduction in symmetry: A study of crystal texture of calcitic sponge spicules. *Chem. Eur. J.* **7**, 414–412.

Austin, B. & Ott, B. 1987 Porifera. In *Marine invertebrates of the Pacific Northwest* (ed. E. N. Kozloff). Seattle: University of Washington Press.

Bavestrello, G. Cattaneo-Vietti, R. Cerrano, C. &. Sara, M.

1993 Rate of spiculogenesis in *Clathrina cerebrum* (Porifera: Calcispongiae) using tetracycline marking. *J. Mar. Biol. Ass. U.K.* **73**, 457–460.

Ebner, V. von 1887 Uber den fieneren bau der skelettheile der kalkschwämme nebst bemerkung uber Kalkskelet überhaupt Sber. *Akad. Wiss. Wien (Abt. I)* **95**, 55–149.

Jones, W. C. 1970 The composition, development, form and orientation of calcareous sponge spicules. In *Biology of the Porifera* (ed. W. Fry). *Symp. zool. Soc. Lond.* **25**, 91–123.

Jones, W. C. 1979 Spicule growth and production in juvenile *Sycon ciliatum*. *In Biologie des spongiaires*, vol. 291 (ed. C. Lévi & N. Boury-Esnault), pp. 67–76. Colloques internationaux du CNRS. Paris: CNRS.

Koehl, M. A. R. 1982 Mechanical design of spicule-reinforced connective tissue: stiffness. *J. exp. Biol.* **98**, 239–267.

Laubenfels, M. W. de 1961 Porifera of Friday Harbor and vicinity. *Pacific Sci.* **15**, 192–202.

Ledger, P. W. Jones, W. C. 1977 Spicule formation in the calcareous sponge *Sycon ciliatum*. *Cell Tiss. Res.* **181**, 553–567.

Ledger, P. W. & Jones, W. C. 1991 On the structure of calcareous sponge spicules. In *Fossil and recent sponges*. (ed. J. Reitner & H. Keupp), 341–359. Berlin: Springer-Verlag.

Levin, L. A. 1990 A review for methods for labeling and tracking marine invertebrate larvae. *Ophelia* **32**, 115–144.

Mann, S., Sparks, N. H. C. & Blakemore, R. P. 1987 Structure, morphology and crystal growth of anisotropic magnetite crystals in magnetotactic bacteria. *Proc. R. Soc. Lond.* B **231**, 477–487.

Mann, S. & Sparks, N. H. C. 1988 Single crystalline nature of coccolith elements of the marine alga *Emiliania huxleyi* as determined by electron diffraction and high-resolution transmission electron microscopy. *Proc. R. Soc. Lond.* B **234**, 441–453.

Minchin, E. A. 1898 Materials for a monograph of the ascons. I On the origin and growth of the triradiate and quadriradiate spicules in the family Clathrinidae. *Q.J. Microsc. Sci.* **40**, 469–587.

Minchin, E. A. 1909 Sponge-spicules. Summary of present knowledge. *Ergebn. Fortschr. Zool.* **2**, 171–274.

Okazaki, K., Dillaman, R. M. & Wilbur, K. M. 1981 Crystalline axes of the spine and test of the sea urchin *Strongylocentrotus purpuratus*: Determination by crystal etching and decoration. *Biol. Bull.* **161**, 402–415.

Ruppert, E. E. & Barnes, R. D. 1994 *Invertebrate zoology*. Fort Worth: Sounders College Publishing.

Simkiss, K. & Wilbur, K. M. 1989 *Biomineralization: cell biology and mineral deposition*. New York: Academic Press.

Strathmann, M. F. 1987 *Reproduction and development of marine invertebrates of the Northern Pacific coast*. Seattle: University of Washington Press.

Received 15 August 1995; accepted 31 October 1995